JOURNAL OF MATERIALS SCIENCE **35** (2000) 1813–1825

# The chemical behaviour of carbon fibres in magnesium base Mg-Al alloys

J. C. VIALA, G. CLAVEYROLAS, F. BOSSELET, J. BOUIX
*Laboratoire des Multimatériaux et Interfaces, UMR CNRS no. 5615, Université Lyon 1, 43 boulevard du 11 Novembre 1918, 69622 Villeurbanne, Cedex, France*
*E-mail: viala@univ-lyon1.fr*

The chemical interaction between carbon fibres and Mg-rich Mg-Al alloys was studied at 723–1273 K using optical metallography, scanning electron microscopy and electron probe microanalysis. In a first stage, carbon fibres were heated at 723, 1000 and 1273 K with Mg-Al alloys of different compositions. Two carbide phases were identified at 1000 and 1273 K: an $Al_4C_3$ type phase with up to 6 wt.%Mg present in solid solution and a new ternary carbide with the chemical formula $Al_2MgC_2$ existing under two hexagonal crystalline varieties. In a second stage, the solid-liquid phase equilibria in the Al-C-Mg ternary system were experimentally established at 1000 K. At that temperature, all the Mg-Al alloys containing more than $19 \pm 2$ wt.%Al were observed to be in equilibrium with the $Al_4C_3$ type phase whereas Mg-Al alloys containing from 0.6 to 19 wt.%Al were found in equilibrium with the ternary carbide $Al_2MgC_2$. As for the Mg-Al alloys with an Al content lower than or equal to $0.6 \pm 0.2$ wt.%, they appeared to be in equilibrium with carbon. These thermodynamic principles being established, the extent, morphology and composition of the reaction zones formed in out of equilibrium conditions at the interface between carbon fibres and Mg-rich Mg-Al alloys were characterized. Attempts were made to determine the influence of different factors such as the fibre nature, the alloy composition, the heating time and the heating temperature on the formation and growth of the ternary carbide $Al_2MgC_2$. The observed changes were interpreted in terms of reaction mechanism and kinetics. 

## 1. Introduction

On the basis of simple theoritical considerations (rule of mixture...) composite materials made of a magnesium base matrix reinforced with continuous carbon or graphite fibres may exhibit a combination of unique properties particularly attractive for aerospace applications [1–6]. First, owing to the low density of magnesium (1.74 instead of 2.7 for aluminium), composites with extremely high specific mechanical properties could be produced. For example, composites made of an AZ61 alloy matrix (6 wt.%Al, 1 wt.%Zn) unidirectionally reinforced with FT700 graphite fibres in a volume fraction of 50% could theoretically possess a longitudinal tensile strength of 1700 MPa and a longitudinal stiffness of 370 GPa for a density of 2. Using highly graphitized fibres should also result in materials with a near zero coefficient of thermal expansion, i.e. with an excellent dimensional stability [2, 7]. Finally, the magnesium matrix should provide to these composites good damping characteristics [8].

Production of materials with the highest possible performances implies, however, a precise control of all factors that may degrade the mechanical properties of the reinforcing fibres and affect the interfacial load transfer. In this regard, a thorough understanding of the chemical reactions likely to develop at the interface between carbon fibres and the magnesium-base matrix during processing or use of these composites is of prime importance.

In a previous study, carbon fibres were shown to exhibit an excellent chemical inertness towards pure magnesium in the temperature range 700–1000 K, provided that these fibres were sufficiently graphitized [9, 10]. This fact being established, it was interesting to examine how this excellent chemical compatibility was affected when aluminium was added to magnesium. Aluminium is effectively present as major addition element in the most common magnesium alloys (from 3 wt.% in the AZ31 alloy to 9 wt.% in the AZ91 alloy) and it is well known that this element can react with carbon and give aluminium carbide $Al_4C_3$. Concerning the occurence of the latter reaction in Mg-Al/carbon fibre composites, the situation was however not very clear. On the one hand, formation of $Al_4C_3$ by reaction of carbon with Mg-Al alloys a priori appeared as highly probable on the basis of simple thermodynamic considerations [11]. On the other hand, this assumption was not fully supported by the observations made at the interface between carbon fibres and Mg-Al alloys. In some cases, no reaction product was found [12–14]. In

other cases, carbide phases attributable to $Al_4C_3$ were found but, due to the low concentration or too small size of the crystals, these phases could not be precisely characterized, even by transmission electron microscopy [15–18] or by Auger electron spectroscopy [19]. Finally, two new crystalline phases corresponding to two polymorphs of a ternary carbide with the chemical formula $Al_2MgC_2$ were shown to exist in the Al-C-Mg system [20].

It is to clear up these different points that the present study was undertaken. In a first approach, attempts were made to characterize the crystalline nature, the morphology and composition of the phases effectively formed by reaction between carbon fibres and Mg-Al alloys at 723, 1000 and 1273 K. Isothermal diffusion experiments were then performed at 1000 K to determine the solid-liquid phase equilibria in the Al-C-Mg ternary system at that temperature. In a third stage, a detailed examination of the reaction zones formed under different experimental conditions at the interface between carbon fibres and Mg-rich Mg-Al alloys was carried out to get more detailed information on the mechanism and kinetics of the fibre/matrix chemical interaction.

## 2. Experimental procedure

Samples used in this study were prepared from commercial powders of magnesium (purity $>98.5$ wt%, grain size $d < 300\,\mu$m, Merck) aluminium (purity 99.8 wt-%, grain size $d < 50\,\mu$m, Alfa), carbon (spectrographic grade, $d < 25\mu$m, Le Carbone Lorraine) and aluminium carbide (stoichiometric $Al_4C_3$, $d < 50\mu$m, Alfa). The powders were ball-milled for 10 min in a tungsten carbide mortar and cold-pressed under 400 MPa into small parallelepiped rods weighing about 2 g ($6 \times 6 \times 30$ mm), using conventional steel tools. Broken pieces ($\approx$1 mm long, 10 $\mu$m in diameter) of pitch base P55 carbon fibres (purity $>99$ wt.%, Amoco) were also employed as carbon source. In that case, the broken fibres were carefully dispersed in previously ball-milled Mg-Al powders (pre-alloyed or not) and the mixtures were cold-pressed under 1.2 GPa into small cylinders weighting about 0.5 g (7 mm high, 7 mm in diameter), using a tungsten carbide compression cell.

The cold-pressed rods and cylinders were isothermally heat-treated under an atmospheric pressure of purified argon (0.1 MPa). At temperatures lower than or equal to 1000 K, we used the experimental closed tube assembly schemed in Fig. 1. This re-usable assembly was designed to avoid a too fast evaporation of magnesium from the mixtures (presence of magnesium powder in excess) and to prevent a rapid degradation of the external silica U tube by magnesium vapour (interposition of an inner iron tube). The samples were placed in a graphite crucible equipped with a cover. It was effectively observed in preliminary experiments that no reaction occurred at the sample/graphite crucible interface, owing to the presence of an MgO oxide scale at the surface of the rods or cylinders. At 1273 K, the vapour pressure of magnesium was too high for operating in the re-usable assembly. Heat-treatments at that temperature were then carried out in iron tubes that were previously

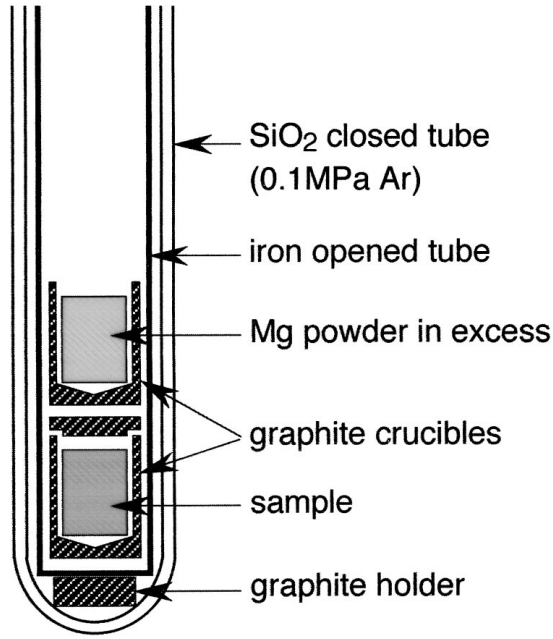


*Figure 1* Re-usable assembly employed for heat-treatments at 1000 K or below.

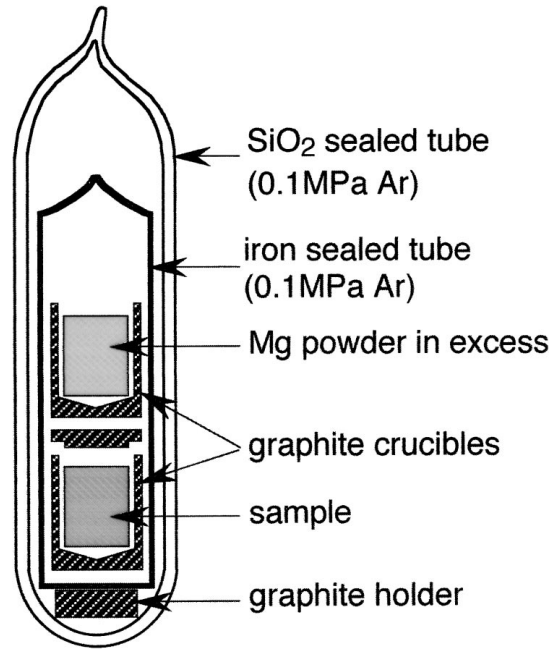


*Figure 2* Sealed tube equipment used for experiments at 1273 K.

sealed under 1 atmosphere of argon and placed inside silica tubes, themselves sealed under 1 atmosphere of argon, as shown in Fig. 2. In both cases, a conventional vertical tube furnace supplied by a stability controller was used as heat source. Although the furnace temperature was regulated within $\pm 3$ K, the accuracy on the sample temperature was no better than $\pm 10$ K. At the end of the isothermal heat-treatments, the assemblies were driven out of the furnace and cooled in air as rapidly as possible.

After having evaluated their weight loss, $-\Delta m/m_0$, the resulting samples were characterized by different techniques. X-ray diffraction (XRD) spectra were systematically recorded on grossly polished faces, using a standard Philips equipment (Ni filtered Cu $K_\alpha$

radiation, $\lambda = 1.54056$ Å). Observations by optical metallography (OM, Olympus Vanox-T microscope) and scanning electron microscopy (SEM, Hitachi S-800 microscope) were made on plane sections that were diamond-polished to a finish of 1 $\mu$m. Further characterization of the phases produced was performed by electron probe microanalysis (EPMA), using a Cameca Camebax apparatus equipped with a wavelength dispersive spectrometer and an energy dispersive analyser. An accelarating voltage of 5 kV, a regulated beam current of about 30 nA and a counting time of 10 s were selected as standard operating parameters. For each phase analysed, the counting rates, $N$, simultaneously recorded for Al and Mg in at least five different points (crystals, punctual mode) or along five different segments 250 $\mu$m long (Mg-Al alloy matrix, line scan mode) were averaged, subtracted for background and referred to the counting rates, $N_0$, recorded under the same conditions for pure Al and Mg standards (also freshly diamond-polished to a finish of 1 $\mu$m). The ratios $N/N_0$ thus obtained were converted into weight contents after correction for atomic number, absorption and fluorescence. The carbon content of the carbide phases was determined by difference, after having verified that no foreign elements were detectable in the fluorescence spectra of these phases. It is worth noting that for obtaining significant values on these carbides which can be very easily hydrolysed, samples containing them must be polished with non-aqueous solvents just before entering the vacuum chamber of the microprobe. Despite this precaution, the relative accuracy on the Al and Mg contents of these phase was not better than about 10%, which resulted in a poor precision on the carbon content determined by difference.

## 3. Characterization of the phases formed by reaction between carbon fibres and Mg-Al alloys

In this first approach, powder mixtures of carbon (broken fibres or particles) aluminium and magnesium (pre-alloyed or not) were cold-pressed, heat-treated and characterized after rapid cooling. Two mixtures were heated at 723 K (450 °C) to investigate the solid state interaction between carbon fibres and single-phased magnesium-rich Mg-Al alloys. Heat-treatments were then carried out at 1000 K (727 °C), temperature at which all the Mg-Al alloys are in the liquid state (Fig. 3). This temperature of 1000 K also corresponds to the upper limit of the range in which aluminium or magnesium base composites are usually processed by liquid phase infiltration. A third series of experiments was carried out at 1273 K (1000 °C) to explore the high temperature domain.

### 3.1. Heat-treatments at 723 K

For these experiments at low temperature, two different Mg-Al alloys were prepared in a first stage: a single-phased Mg-based alloy containing 6 wt.%Al and a single-phased alloy of the compound $Al_{12}Mg_{17}$ containing 43.9 wt.%Al. It can be seen in Fig. 3 that both alloys are in the solid state at 723 K (450 °C). Mixtures made of powders of each of these two alloys with a few

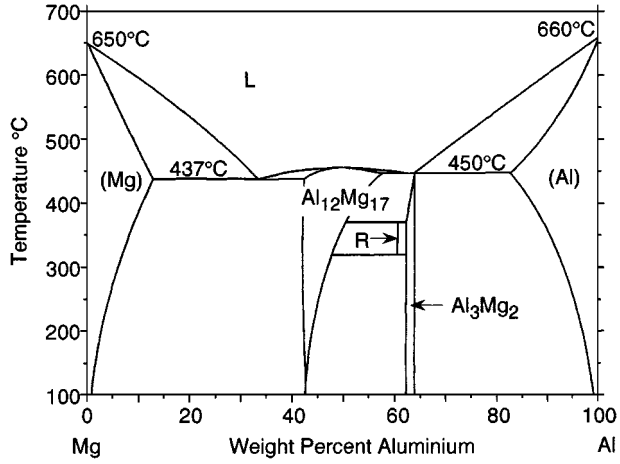


*Figure 3* The Al-Mg binary phase diagram [21].

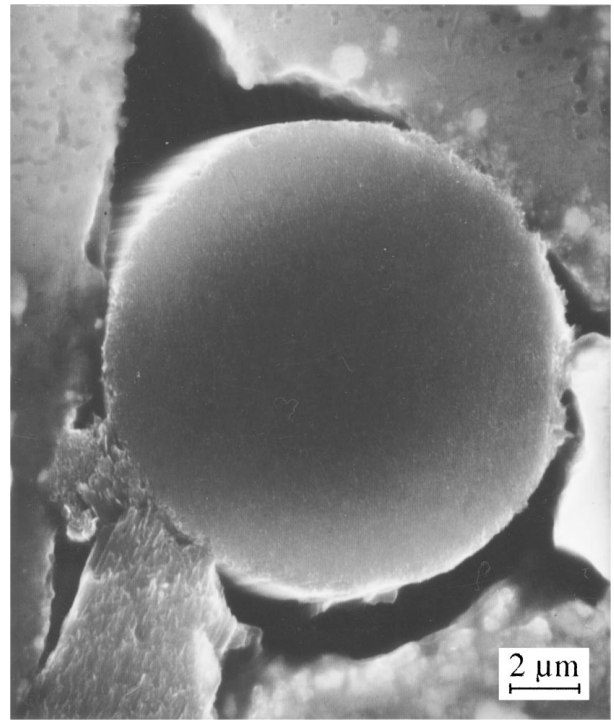


*Figure 4* SEM photograph showing the interface between a P55 carbon fibre and a Mg-Al 6 alloy after heating for 1200 hours at 723 K: no solid state interaction observable.

broken P55 carbon fibres (1.6 wt.%) were then cold-pressed, heated at 723 K for 1200 hours and rapidly cooled. In spite of the very long duration of the heat-treatment, no indication of solid state reaction could be found at the interface between the fibres and the Mg-Al alloys. Most often, the fibres appeared inserted between three grains of the Mg-Al matrix, touching them only in rare points, as shown in Fig. 4. The EPMA concentration profiles recorded in these points (Fig. 5) were characteristic for an abrupt interface, the width of the fibre/matrix transition zone (about 2.5 $\mu$m) corresponding to the lateral resolution of the technique under the operating conditions used.

### 3.2. Heat-treatments at 1000 K

In this second series of experiments, carbon particles and P55 broken fibres were heated for 60 hours at 1000 K under an atmospheric pressure of argon

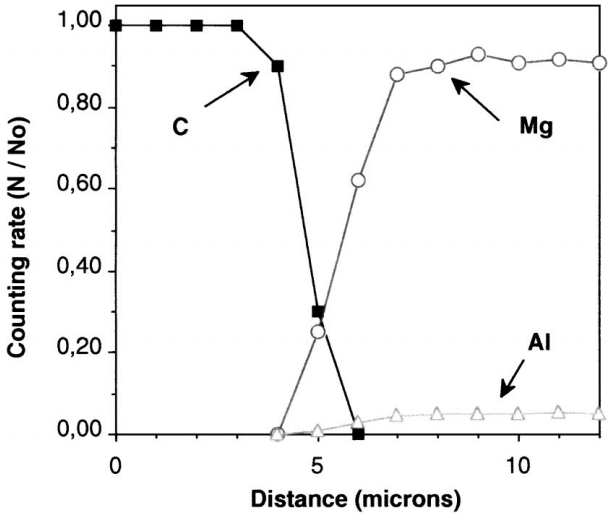


*Figure 5* EPMA concentration profiles recorded for Al, C and Mg at the crossing of the interface between a P55 carbon fibre and a Mg-Al 6 alloy after 1200 hours heating at 723 K, showing an abrupt interface (the counting rates $N/N_0$ are referred to pure Al, C and Mg standard).

(0.1 MPa) with Mg-Al liquid alloys having the following initial Al contents: 50, 30, 15 and 6 wt.%Al. Prealloying magnesium and aluminium powders appeared useless since a homogeneous liquid alloy was formed in few minutes after melting. X-ray studies were carried out on rods (cold-pressed under 400 MPa) containing initially rather large amounts of carbon in the form of graphite powder (10 to 20 wt.%C). OM or SEM observations and EPMA analyses were performed on small cylinders (cold-pressed under 1200 MPa) containing broken P55 carbon fibres in much smaller proportion, (2.4 wt.%C). For all these samples, the weight loss was lower than 20%.

Results obtained by XRD are summarized in Table I. The first observation that could be made was that all the samples treated at 1000 K mainly consisted of unreacted graphite and of a solidified Mg-Al alloy, the composition of which was not very different from the starting one: in fact, only a moderate enrichment of the alloy in magnesium occurred, indicating that reactions between graphite and the Mg-Al alloys under the experimental conditions used were very incomplete.

Despite the incomplete character of the reactions and the presence of magnesium oxide impurity (brought with the starting Mg powder), the aluminium carbide phase, $Al_4C_3$, could be unambiguously characterized by XRD as reaction product in the two samples where graphite had been heated in the presence of the Mg-Al alloys with the highest aluminium contents (samples Mg-Al 50/$C_{gr}$ and Mg-Al 30/$C_{gr}$). The characteristic diffraction lines of this reaction product appeared, however, at angular positions slightly different from those reported for pure $Al_4C_3$ in the JCPDS diffraction file 35-799. Using a classical least square program, the unit cell parameters of the carbide formed by reaction were refined in a hexagonal symmetry. To the precision the method used, the values obtained for the cell parameter, $a$, corresponded to that of 3.3388(3) Å reported for pure $Al_4C_3$ in the above mentioned diffraction file whereas the values obtained for the cell parameter, $c$, were slightly larger: $c = 25.11(3)$ Å for sample Mg-Al 50/$C_{gr}$ or $c = 25.16(3)$ Å for sample Mg-Al 30/$C_{gr}$ instead of $c = 24.996(3)$ Å for pure $Al_4C_3$. Examination by OM of the small corresponding cylinders Mg-Al 50/P55 and Mg-Al 30/P55 revealed the same typical morphology for the $Al_4C_3$ phase produced. As shown in Fig. 6, this phase formed elongated crystals (platelets) up to 10 $\mu$m long protruding from the surface of the fibres into the Mg-Al matrix. The composition of these crystals, as determined by EPMA in samples Mg-Al 50/P55 and Mg-Al 30/P55 (Table II), was found consistent with that of an $Al_4C_3$ phase in which 5 to 6 wt.% of magnesium were present. As suggested by the values in at.% reported between brackets in Table II, magnesium atoms might replace aluminium atoms in the structure of $Al_4C_3$.

For the two Mg-Al/$C_{gr}$ samples the richest in magnesium (Mg-Al 15/$C_{gr}$ and Mg-Al 6/$C_{gr}$), no reaction product could be characterized by XRD, due the too strong intensity of the diffraction lines of metallic magnesium, whereas a reaction phase was clearly revealed

TABLE I Phases characterized by XRD in Mg-Al/$C_{gr}$ samples heat-treated at 1000 K for 60 hours under 0.1 MPa of argon and in the presence of Mg vapour in excess

| Sample | Initial composition wt.%Mg | wt.%Al | wt.%C | Phases characterized by XRD (decreasing abundance) |
|---|---|---|---|---|
| Mg-Al 50/$C_{gr}$ | 40 | 40 | 20 | $Al_{12}Mg_{17}$, C, $Al_4C_3$,MgO |
| Mg-Al 30/$C_{gr}$ | 60.9 | 26.1 | 13 | $Mg_{sol.sol.}$, $Al_{12}Mg_{17}$, C, MgO, $Al_4C_3$ |
| Mg-Al 15/$C_{gr}$ | 76.5 | 13.5 | 10 | $Mg_{sol.sol.}$, C, $Al_{12}Mg_{17}$, MgO |
| Mg-Al 6/$C_{gr}$ | 83.6 | 5.3 | 11 | Quasi-pure Mg, C, MgO |

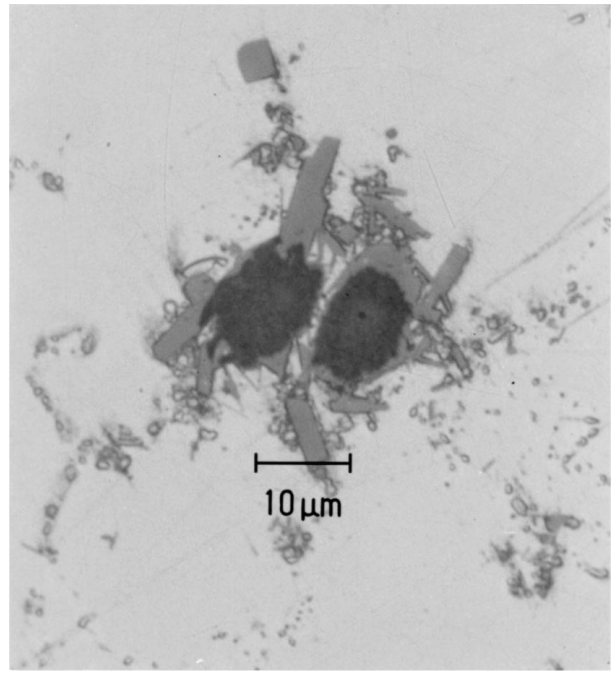


*Figure 6* Optical micrograph of the Mg-Al 30/P55 interface after 60 hours heating at 1000 K. $Al_4C_3$ hexagonal platelets protrudes from the fibre surface into the Mg-Al matrix.

TABLE II Composition in wt.% (and corresponding values in at.%) of the carbide crystals formed in Mg-Al/P55 samples after 60 hours heating at 1000 K under 0.1 MPa of argon

| Sample | Composition and nature of the reaction carbide crystal | | | |
|---|---|---|---|---|
| | wt.%Mg (at.%Mg) | wt.%Al (at.%Al) | wt.%C (at.%C) | |
| Mg-Al 50/P55 | 4.9 | 70.4 | 24.7 | $Al_4C_3$ |
| | (4.1) | (53.7) | (42.2) | (XRD) |
| Mg-Al 30/P55 | 6.0 | 69.4 | 24.6 | $Al_4C_3$ |
| | (5.1) | (52.8) | (42.1) | (XRD) |
| Mg-Al 15/P55 | 22.6 | 50.6 | 26.8 | $Al_2MgC_2$ |
| | (18.5) | (37.2) | (44.3) | |
| Mg-Al 6/P55 | 23.4 | 51.6 | 25.0 | $Al_2MgC_2$ |
| | (19.5) | (38.7) | (41.8) | |

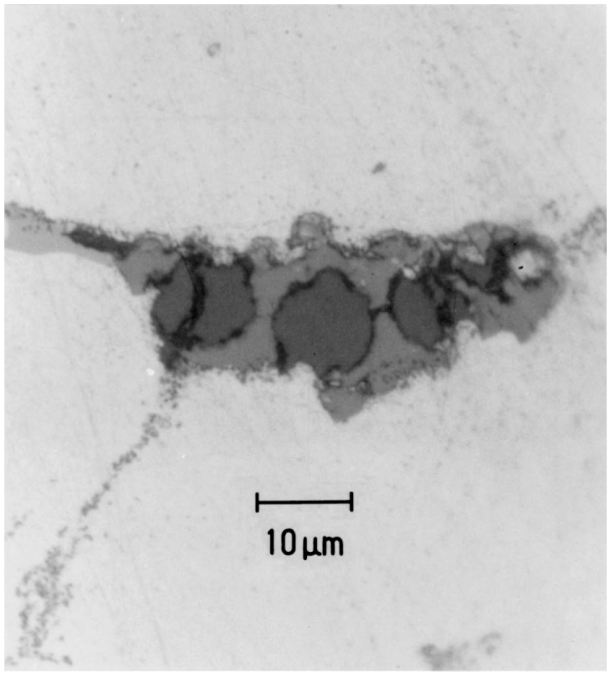


*Figure 7* Globular $Al_2MgC_2$ crystals formed after 60 hours heating at 1000 K at the interface between P55 carbon fibres and Mg-rich Mg-Al alloys.

at the interface between the P55 fibres and the alloy by OM observation of the corresponding magnesium rich Mg-Al 15/P55 and Mg-Al 6/P55 cylinders. On the one hand, this reaction phase underwent a rapid hydrolysis in ambient air, as $Al_4C_3$, but on the other hand, its morphology was different from that of $Al_4C_3$. As shown in Fig. 7, the reaction product effectively appeared rather in the form of globular crystals than in that of elongated ones. Furthermore, EPMA analyses of this reaction phase in Mg-Al 15/P55, Mg-Al 6/P55 cylinders revealed Al, C and Mg contents that were incompatible with any known phase of the Al-C-Mg system (Table II).

To solve the XRD characterization problem, the duration of the heat-treatment of the magnesium-rich Mg-Al/$C_{gr}$ cold-pressed rods was increaed by steps from 60 to 200 hours, the pressure of argon in the reaction tube was reduced from $10^5$ to $3.8 \times 10^4$ Pa and excess magnesium powder was not added. This resulted in a slow evaporation of magnesium from the samples during the whole course of the heat-treatment, the relative weight loss for this metal, $-\Delta m/m_0$, being of about 0.45% by hour.

TABLE III Composition in wt.% (and corresponding values in at.%) of the carbide crystals formed in Mg-Al/$C_{gr}$ samples after 60 hours heating at 1000 K under a reduced pressure of argon ( LP = 0.038 MPa) and without Mg in excess

| Sample | Composition and nature of the reaction carbide crystals | | | |
|---|---|---|---|---|
| | Mg wt.% (at.%) | Al wt.% (at.%) | C wt.% (at.%) | |
| Mg-Al 15/$C_{gr}$ (LP) | 24.4 | 49.4 | 26.1 | $Al_2MgC_2$ |
| | (20) | (36.6) | (43.4) | Form T1 (XRD) |
| Mg-Al 6/$C_{gr}$ (LP) | 22.1 | 50.1 | 27.8 | $Al_2MgC_2$ |
| | (17.9) | (36.5) | (45.6) | Form T1 (XRD) |

After 60 hours heating under these new experimental conditions (LP), globular crystals with the same composition as those previously obtained were observed by OM and analysed by EPMA in samples Mg-Al 15/$C_{gr}$(LP) and Mg-Al 6/$C_{gr}$(LP) (Table III). Moreover, owing to the evaporation of magnesium, a new set of diffraction lines became visible in the XRD spectrum of these samples. As no phase with this set of lines was reported so far in the Al-C-Mg system, it was concluded that a new aluminium-magnesium carbide had been synthesized. On the basis of theoretical considerations and referring to EPMA results, we have attributed to this ternary carbide the chemical formula $Al_2MgC_2$ [20].

After 180–200 hours heating, all the metallic magnesium had disappeared from the samples Mg-Al 15/$C_{gr}$(LP) and Mg-Al 6/$C_{gr}$(LP), which allowed a precise determination of the angular position and intensity of the diffraction lines of the first set characteristic for $Al_2MgC_2$. These lines were indexed in a hexagonal symmetry with $a = 3.4017(7)$ and $c = 12.292(2)$ Å (crystalline phase $T_1$, Table IV). However, heating for 200 hours under reduced pressure also revealed a second set of unknown diffraction lines. This second set which appeared superimposed on the first set was also indexed in a hexagonal symmetry with $a = 3.377(1)$ and $c = 5.817(4)$ Å (crystalline phase $T_2$, Table V).

At this stage of the heat-treatment, not one but two new crystalline phases were present with MgO and unreacted carbon in the magnesium-rich Mg-Al/$C_{gr}$ samples. The question was to determine the composition of the crystalline phase $T_2$ mixed with $Al_2MgC_2$ crystals of the $T_1$ variety. It was thought for a moment that $T_2$ crytals could form by decomposition of $Al_2MgC_2$, as a consequence of magnesium evaporation during prolonged heating, but this hypothesis had to be ruled out. Effectively, no appreciable change occurred in the XRD spectrum of sample Mg-Al 15/Cgr(LP) previously treated for 200 hours at 1000 K on re-heating for 65 hours at 1000 K under a primary vacuum of 10 Pa: the only conclusion that could be drawn was that the ternary carbide $Al_2MgC_2$ with the crystalline form $T_1$ was stable at 1000 K under vacuum. In fact, additional experiments carried out at 1273 K revealed that the crystalline phases $T_1$ and $T_2$ had the same composition.

TABLE IV X-ray powder diffraction data for the ternary carbide $Al_2MgC_2$ under the crystalline form $T_1$ (hexagonal crystal symmetry with $a = 3.4017(7)$ and $c = 12.292(2)$ Å, filtered Cu $K_\alpha$ radiation $\lambda = 1.54056$ Å)

| $d_{obs.}$ (Å) | $d_{calc.}$ (Å) | $h$ | $k$ | $I$ | $I/I_{0\,obs.}$ |
|---|---|---|---|---|---|
| 6.156 | 6.146 | 0 | 0 | 2 | 18 |
| 3.071 | 3.073 | 0 | 0 | 4 | 17 |
| — | 2.946 | 1 | 0 | 0 | —[a] |
| 2.864 | 2.864 | 1 | 0 | 1 | 100 |
| 2.655 | 2.656 | 1 | 0 | 2 | 48 |
| 2.390 | 2.392 | 1 | 0 | 3 | 70 |
| 2.125 | 2.126 | 1 | 0 | 4 | 62 |
| 2.047 | 2.049 | 0 | 0 | 6 | 46 |
| 1.8863 | 1.8874 | 1 | 0 | 5 | 33 |
| 1.7003 | 1.7006 | 1 | 1 | 0 | 69 |
| — | 1.6819 | 1 | 0 | 6 | —[a] |
| 1.6387 | 1.6391 | 1 | 1 | 2 | 3 |
| — | 1.5365 | 0 | 0 | 8 | <2 |
| 1.5081 | 1.5083 | 1 | 0 | 7 | 6 |
| — | 1.4880 | 1 | 1 | 4 | —[a] |
| — | 1.4728 | 2 | 0 | 0 | — |
| — | 1.4623 | 2 | 0 | 1 | —[a] |
| 1.4321 | 1.4320 | 2 | 0 | 2 | 7 |
| 1.3860 | 1.3860 | 2 | 0 | 3 | 10 |
| 1.3625 | 1.3623 | 1 | 0 | 8 | 8 |
| 1.3280 | 1.3281 | 2 | 0 | 4 | 10 |
| 1.3077 | 1.3085 | 1 | 1 | 6 | 38[a] |
| — | 1.2634 | 2 | 0 | 5 | —[a] |
| 1.2390 | 1.2390 | 1 | 0 | 9 | 6 |
| — | 1.2292 | 0 | 0 | 10 | —[a] |
| 1.1955 | 1.1958 | 2 | 0 | 6 | 2 |
| — | 1.1401 | 1 | 1 | 8 | — |
| 1.1342 | 1.1344 | 1 | 0 | 10 | 3 |

[a]These reflexions may be hidden by other lines from MgO, C, $T_2$.

TABLE V X-ray powder diffraction data for the ternary carbide $Al_2MgC_2$ under the crystalline form $T_2$ (hexagonal crystal symmetry with $a = 3.377(1)$ and $c = 5.817(4)$ Å, filtered Cu $K_\alpha$ radiation $\lambda = 1.54056$ Å)

| $d_{obs.}$ (Å) | $d_{calc.}$ (Å) | $h$ | $k$ | $I$ | $I/I_{0\,obs.}$ |
|---|---|---|---|---|---|
| 5.824 | 5.817 | 0 | 0 | 1 | 5 |
| 2.924 | 2.925 | 1 | 0 | 0 | 10 |
| — | 2.908 | 0 | 0 | 2 | —[a] |
| 2.612 | 2.613 | 1 | 0 | 1 | 100 |
| 2.062 | 2.062 | 1 | 0 | 2 | 68 |
| 1.9385 | 1.9389 | 0 | 0 | 3 | 17 |
| 1.6887 | 1.6887 | 1 | 1 | 0 | 43 |
| — | 1.6217 | 1 | 1 | 1 | — |
| 1.6162 | 1.6161 | 1 | 0 | 3 | 7 |
| 1.4617 | 1.4625 | 2 | 0 | 0 | 5 |
| — | 1.4604 | 1 | 1 | 2 | — |
| — | 1.4542 | 0 | 0 | 4 | — |
| 1.4185 | 1.4183 | 2 | 0 | 1 | 15 |
| 1.3077 | 1.3066 | 2 | 0 | 2 | 15[a] |
| — | 1.3021 | 1 | 0 | 4 | 8[a] |
| 1.2736 | 1.2734 | 1 | 1 | 3 | 19 |
| 1.1670 | 1.1676 | 2 | 0 | 3 | 1 |
| — | 1.1633 | 0 | 0 | 5 | — |

[a]These reflexions may be hidden by other lines from MgO, C, $T_1$.

## 3.3. Heat-treatments at 1273 K

As previously remarked, only very incomplete reactions were generally observed after 65 hours heating at 1000 K. To favour a more pronounced chemical interaction and characterize further the reaction products, a third series of heat-treatments was performed at 1273 K on various mixtures of the Al-C-Mg system, using the experimental assembly illustrated schematically in Fig. 2. In that case, the heating duration was of 10 hours (for longer reaction times, the tightness of the heating assembly was no more ensured). Results obtained by XRD and EPMA for this third series of high temperature experiments, summarized in Table VI, were effectively very different from those previously reported after 65 hours heating at 1000 K.

TABLE VI Phases characterized by XRD in Mg-Al/$C_{gr}$ and Mg-Al/P55 samples reacted for 10 hours at 1273 K in a sealed iron tube

| Sample | Initial composition wt.%Mg | wt.%Al | wt.%C | Phases characterized by XRD (decreasing abundance) |
|---|---|---|---|---|
| Mg-Al 82/$C_{gr}$ | 10.8 | 48.6 | 40.6 | $T_2$, C, $Al_4C_3$, MgO |
| Mg-Al 73/$C_{gr}$ | 21 | 57 | 22 | $T_2$, $Mg_{sol.sol.}$, $Al_4C_3$, MgO, C |
| Mg-Al 53/$C_{gr}$ | 35 | 39 | 26 | $T_2$, quasi-pure Mg, C, MgO, $Al_4C_3$ |
| Mg/$C_{gr}$ + $Al_4C_3$ | 35 | 39 | 26 | Quasi-pure Mg, $Al_4C_3$, MgO, $T_2$, C |
| Mg-Al 14.3/$C_{gr}$ | 66 | 11 | 23 | Quasi-pure Mg,$T_2$, C, MgO, $Al_4C_3$ |
| Mg-Al 14.3/P55 | 75.1 | 12.5 | 2.4 | $Mg_{sol.sol.}$, MgO, $Al_{12}Mg_{17}$ |
| Mg-Al 2/P55 | 95.65 | 1.95 | 2.4 | Quasi-pure Mg, MgO |

It first appeared that, contrarily to what was observed at 1000 K, the Mg-Al alloys present in the samples after heating for 10 hours at 1273 K were quite different in composition from the starting ones. For sample Mg-Al 82/$C_{gr}$, all the metallic magnesium initially present was combined (no metallic or intermetallic Al-Mg phase was detectable). For sample Mg-Al 73/$C_{gr}$, a magnesium-rich alloy remained (Mg-Al 12 from EPMA results). For samples Mg-Al 53/$C_{gr}$ and Mg-Al 14.3/$C_{gr}$, all the aluminium initially present was combined and quasi-pure magnesium was the only metallic phase characterized after reaction. Another important difference was the fact hat the three samples initially the richest in aluminium, i.e. samples Mg-Al 82/$C_{gr}$, Mg-Al 73/$C_{gr}$ and Mg-Al 53/$C_{gr}$ all contained the crystalline phase $T_2$, phase which had not been detected after 65 hours at 1000 K. In addition to this phase $T_2$, an $Al_4C_3$ type phase with a slightly shifted $c$ parameter was also characterized, as at 1000 K, but the relative abundance of the latter was much lower than that of the former.

From these results, it was obvious that reactions had progressed much farther during the 10 hours heating at 1273 K than during the 65 hours heating at 1000 K. However, it was also clear that equilibrium was generally not reached since more than three phases (in addition to MgO impurity) were found in samples Mg-Al 73/$C_{gr}$, Mg-Al 53/$C_{gr}$ and Mg-Al 14.3/$C_{gr}$. Effectively, no more than three phases are generally obtained in a ternary system under a constant pressure when equilibrium is reached at a given temperature (obtaining four phases is not theoretically impossible but the choosen temperature would have to corespond exactly to that of an invariant transformation, which is

very unlikely). In the same regard, the relative abundance of the constituents in samples Mg-Al 53/$C_{gr}$ and Mg/$C_{gr}$ + $Al_4C_3$ were found very different after reaction at 1273 K whereas these two samples had initially the same elemental composition. Why equilibrium conditions could not be attained at a reaction temperature as high as 1273 K could of course be justified by bad quality contacts between the reactants or by graphite passivation. In fact, the main reason was else, as revealed by the results obtained for sample Mg/$C_{gr}$ + $Al_4C_3$, which showed that a reaction between $Al_4C_3$ and pure magnesium yielding the crystalline phase $T_2$ was possible but progressed at a very slow rate. The non-attainment of equilibrium at 1273 K could thus be understood by considering that $Al_4C_3$ was rapidly formed in a first stage of the interaction and had not time enough to react with magnesium in a second stage.

Examination by OM and SEM of polished sections of samples Mg-Al 73/$C_{gr}$ and Mg-Al 53/$C_{gr}$ revealed that at 1273 K, the reaction phases $Al_4C_3$ and $T_2$ formed facetted platelets imbricated in each other (Fig. 8). Analyses performed by EPMA on sample Mg-Al 73/$C_{gr}$ yielded two different sets of values for Al, C and Mg: a first set attributable to the $Al_4C_3$ phase (with about 6 wt.% of magnesium in solid solution) and a second set corresponding to the crystalline phase $T_2$. As shown by Table VII, the composition found for this crystalline phase $T_2$ was, to the precision of the technique used, the same as that previously established for the crystalline phase $T_1$. The same phase composition was also obtained by EPMA for the crystals formed after 10 hours heating at 1273 K in sample Mg-Al 14.3/P55: in that case, $Al_4C_3$ was not found and the final alloy composition was of 11 wt.%Al. Finally, no indication of the formation of a reaction product was obtained for sample Mg-Al 2/P55: only a slight variation in the aluminium content of the alloy could be detected from 2 to 2.6 wt.%Al.

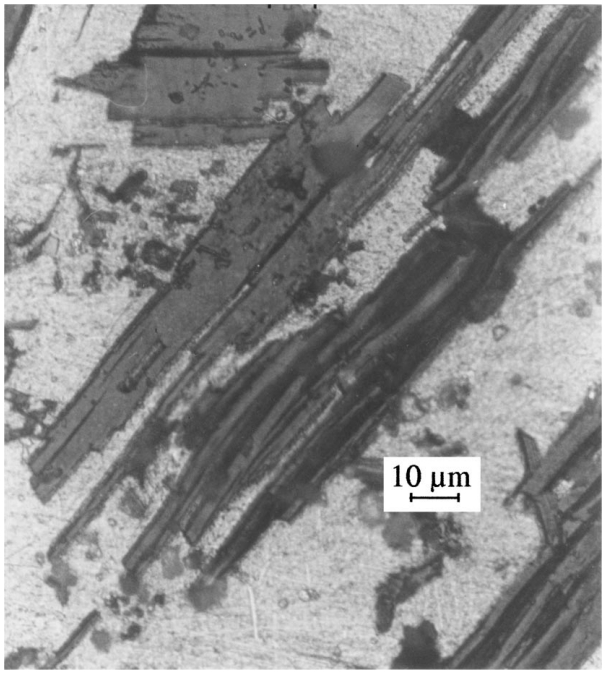


*Figure 8* Optical micrograph of sample Mg-Al 73/$C_{gr}$ after 10 hours heating at 1273 K showing $Al_4C_3$ (dark) and $Al_2MgC_2$ (grey) platelets of the $T_2$ variety imbricated in each other.

TABLE VII Composition in wt.% (and corresponding values in at.%) of the carbide crystals formed in samples Mg-Al 73/$C_{gr}$ and Mg-Al 14.3/P55 after 10 hours heating at 1273 K in a sealed iron tube

| | Composition and nature of the reaction carbide phase | | | |
|---|---|---|---|---|
| Sample | wt.%Mg (at.%Mg) | wt.%Al (at.%Al) | wt.%C (at.%C) | |
| Mg-Al 73/$C_{gr}$ | 6.7 | 69.3 | 24 | $Al_4C_3$ |
| | (5.7) | (53.1) | (41.2) | (XRD) |
| ” | 20.8 | 50 | 29.2 | $Al_2MgC_2$ |
| | (16.7) | (36.1) | (47.2) | Form $T_2$(XRD) |
| Mg-Al 14.3/P55 | 22.7 | 53.6 | 23.7 | $Al_2$ $MgC_2$ |
| | (19) | (40.6) | (40.4) | |

At this point, it was logical to consider that the crystalline phases $T_1$ and $T_2$ were two polymorphs of the same aluminium-magnesium ternary carbide with the chemical formula $Al_2MgC_2$, $T_1$ appearing rather as a “low temperature” variety and $T_2$ rather as a “high temperature” variety. To acquire more detailed information on the thermal stability of these two polymorphs, sample Mg-Al 15/Cgr(LP, 200 hours heating) in which $Al_2MgC_2$ under the $T_1$ and $T_2$ crystalline varieties had formed at 1000 K was re-heated for 10 hours at 1273 K and sample Mg-Al 53/$C_{gr}$ in which only the $T_2$ crystalline variety of $Al_2MgC_2$ had formed at 1273 K was re-heated for 65 hours at 1000 K. XRD characterization of the resulting products did not show any transformation between the “low” and “high temperature” varieties: $T_1$ was not changed into $T_2$ on reheating at 1273 K and $T_2$ was not changed into $T_1$ on re-heating at 1000 K. The two varieties $T_1$ and $T_2$ would then exhibit certain metastable character, like for instance the $\beta$-cubic and $\alpha$-hexagonal crystalline forms of silicon carbide SiC.

## 4. Phase equilibria at 1000 K in the Al-C-Mg system

It was noticed in the preceding Section that reactions in the Al-C-Mg system were very often incomplete, even at temperatures as high as 1273 K, which impeded attainment of equilibrium. The only equilibria that could be considered as being established at 1000 or 1273 K were local equilibria between liquid Mg-Al alloys and crystals of $Al_4C_3$ or $Al_2MgC_2$ growing from these alloys as a result of the attack of carbon particles or fibres. In order to acquire more detailed information on the phase relations in the Al-C-Mg system, a further study of these solid-liquid phase equilibria was carried out by isothermal diffusion at 1000 K, i.e. at the highest temperature still compatible with the production of Mg-Al base composites by liquid phase processing.

Two conditions had to be fulfilled for obtaining significant results: first, the composition of the liquid alloys must not vary in large proportions during the whole length of the heat-treatment and second, the carbide crystals growing from the liquid must be large enough for a non-ambiguous characterization by

TABLE VIII Alloy matrix and carbide crystals compositions, as determined by EPMA in Mg-Al/P55 samples (2.4 wt.%C) after heating for 60–65 hours at 1000 K

| Mg-Al/P55 sample no. | Aluminium content in the Mg-Al alloy matrix | | Composition of the crystalsformed by reaction | | |
|---|---|---|---|---|---|
| | wt.%Al (initial) | wt.%Al (final) | wt.%Mg | wt.%Al | wt.%C[a] |
| 1 | 75 | $70 \pm 4$ | 4.5 | 73.6 | 21.9 |
| 2 | 50 | $49 \pm 3$ | 4.9 | 70.5 | 24.6 |
| 3 | 40 | $43 \pm 3$ | 4.6 | 71.7 | 23.7 |
| 4 | 30 | $31 \pm 3$ | 6.0 | 71.0 | 23.0 |
| 5 | 23 | $22 \pm 2.5$ | 6.1 | 70.9 | 23.0 |
| 6 | 21 | $23 \pm 2.5$ | 5.6 | 67.7 | 26.7 |
| 7 | 19 | $21 \pm 2.5$ | 5.1 | 68.3 | 26.6 |
| 8 | 17 | $19 \pm 2.5$ | 21.4 | 51.2 | 27.4 |
| 9 | 15 | $16 \pm 2$ | 22.6 | 50.6 | 26.8 |
| 10 | 14.3 | $16 \pm 2$ | 26.4 | 49.8 | 23.8 |
| 11 | 6 | $5 \pm 1$ | 23.4 | 51.6 | 25.0 |
| 12 | 2.5 | $1.5 \pm 0.5$ | 23.8 | 52.0 | 24.2 |
| 13 | 2 | $0.6 \pm 0.2$ | 21.8 | 50.7 | 27.5 |
| 14 | 2[b] | $0.7 \pm 0.2$ | 22.6 | 49.6 | 27.8 |
| 15 | 0.5 | $0.6 \pm 0.2$ | — | — | — |

[a]Calculated by difference to 100%.
[b]130 hours heating.

EPMA. Practically, these ideal conditions could be approached by heating Mg-Al/C samples for 60–65 hours at 1000 K in the assembly shown in Fig. 1. For these experiments, the opened crucible filled with pure magnesium powder was placed above the covered crucible containing the samples and the heat-treatments were realized under an atmospheric pressure of argon. Each sample was a small cylinder prepared by cold-pressing under 1200 MPa a mixture of magnesium and aluminium powders (not pre-alloyed) in which broken P55 carbon fibres had been dispersed. The aluminium content of the initial Al-Mg mixture varied from 0.5 to 75 wt.%Al depending on the sample; the proportion of the P55 broken fibres added was fixed at a value of 2.4 wt.% (Table VIII, samples no. 1 to 15).

After 60–65 hours heating at 1000 K and rapid cooling, carbide crystals with a thickness of at least 2 $\mu$m were found at the fibre/matrix interface in all the treated Mg-Al/P55 samples except the one the richest in magnesium (Table VIII, sample 15). These crystals could then be easily characterized by EPMA (point mode). The weight loss of the samples was evaluated to be less than 20%. This weight loss was in fact very difficult to measure precisely since condensed magnesium droplets in variable amounts were often stuck to the surface of the samples. To overcome this problem, the composition of the Mg-Al alloy matrix was systematically re-determined by EPMA (line scan mode) after heat-treatment. The results obtained are reported in Table VIII.

As concerns the Mg-Al alloy matrix, EPMA did not reveal any significant variation before and after heat-treatment as long as the initial aluminium content of the Mg-Al powder mixture constituting the major part of the samples was higher than or equal to 6 wt.% (samples 1 to 11). For these samples, enrichment of the alloy matrix in aluminium due to magnesium evaporation was, to a certain extent, counterbalanced by impoverishment due to reaction with carbon. This was no more true for samples 12–14 in which a significant impoverishment in aluminium of the Mg-Al matrix was detected. It is worth noting that for samples 13 and 14, the aluminium content of the Mg-Al matrix decreased from an initial value of 2 wt.% to a final value of 0.6–0.7 wt.% whatever the heating time, whereas for sample 15 in which no reaction occured, this aluminium content remained unchanged or slightly increased from an initial value of 0.5 wt.% to a final value of $0.6 \pm 0.2$ wt.%.

Concerning the carbide crystals analyzed in all the treated samples except sample 15, they could be classed in two groups. Crystals grown in Mg-Al matrices with an aluminium content higher than or equal to 19 wt.% exhibited compositions characteristic for an $Al_4C_3$ type binary carbide with up to 6 wt.% of magnesium present in solid solution. Crystals grown in Mg-Al matrices with an aluminium content ranging from 0.6 to 19 wt.% had compositions typical for the ternary aluminium-magnesium carbide $Al_2MgC_2$ previously characterized.

Exploitation of these results in terms of liquid-solid equilibria led to the construction of the Al-C-Mg isothermal section presented in Fig. 9. Two three-phase equilibria are remarkable in this section. These are on the one hand the equilibrium between carbon, the ternary carbide $Al_2MgC_2$ and a Mg-Al liquid containing $0.6 \pm 0.2$ wt.%Al ($0.54 \pm 0.2$ at.%Al) and on the other hand, the equilibrium between the ternary carbide $Al_2MgC_2$, the binary carbide $Al_4C_3$ with about 6 wt.%Mg in solid solution and a Mg-Al liquid containing $19 \pm 2$ wt.%Al ($17.5 \pm 2$ at.%Al). In the absence of any other ternary phase, the equilibrium between the three solid phases C-$Al_2MgC_2$-$Al_4C_3$ deduces by construction.

Indications on how the Al-C-Mg phase equilibria experimentally determined at 1000 K may change when the temperature decreases are given in Fig. 10. This tentative representation based on simple thermodynamic considerations shows that the phase fields of carbon and of $Al_2MgC_2$ become narrower when the Mg-Al alloy changes from a liquid to a solid. Consequently, Mg-Al alloys with an aluminium content as low as 0.1 wt.% would react in the solid state with carbon. From 0.1

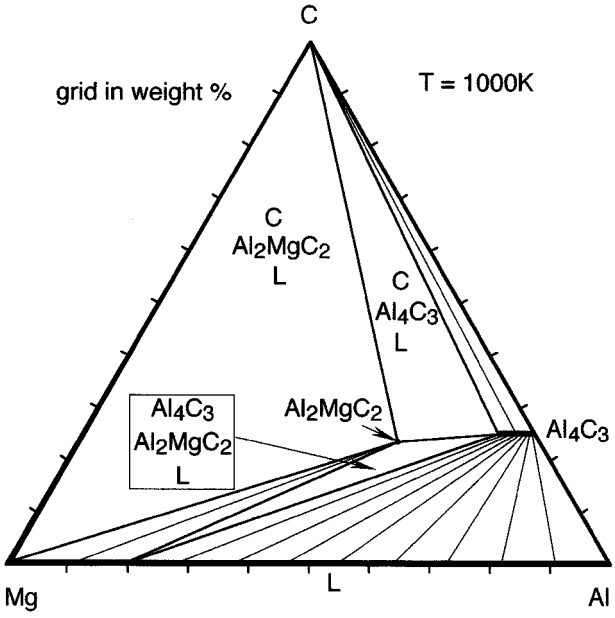


*Figure 9* Phase equilibria at 1000 K in the Al-C-Mg sytem ($P$ = 0.1 MPa).

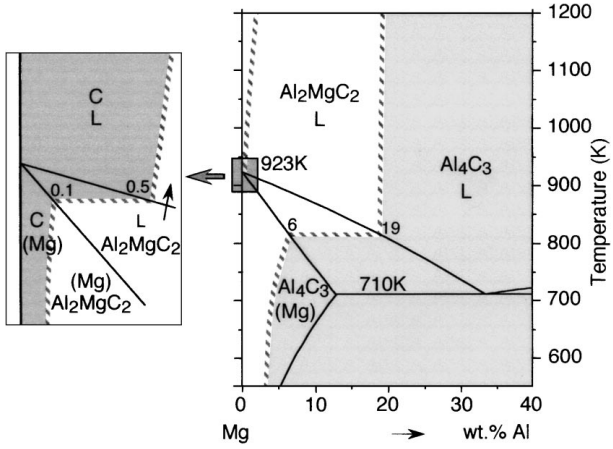


*Figure 10* Tentative representation of the Al-C-Mg phase equilibria below 1000 K.

to about 6 wt.%Al, it is the ternary carbide $Al_2MgC_2$ (under the crystalline form $T_1$) that would be produced by solid state reaction while for aluminium contents higher than about 6 wt.%, $Al_4C_3$ would appear.

## 5. Mechanism and kinetics of growth of the ternary carbide $Al_2MgC_2$

In the scope of producing high performance magnesium base matrix composites, it was interesting to get a better insight into the mechanism and kinetics of growth of the ternary carbide $Al_2MgC_2$ by reaction between carbon fibres and magnesium-rich Mg-Al alloys. For that purpose, heat-treatments were carried out in the temperature range 723–1000 K on small cylinders prepared by cold-pressing broken carbon fibres (2.4 wt.%) with Mg-Al powder mixtures of different compositions (from 2 to 10 wt.%Al). After having verified by EPMA that the composition of the crystals formed by reaction effectively corresponded to that of the ternary carbide $Al_2MgC_2$, attention was focussed on the morphology of the metal/fibre interface and its evolutions with the heating time, the heating temperature, the alloy composition and the fibre nature.

The SEM photographs presented in Fig. 11a to d illustrate the development of the interface reaction in Mg-Al 2.5/P55 samples heat-treated at 930 K. After 10 hours heating (Fig. 11a), only some places of the carbon fibre surface have effectively been wetted by the liquid alloy, suggesting that an induction period is needed to break protective oxide layers. In these places where an intimate contact has established, carbon has begun to dissolve in the liquid alloy, leaving the small depressions visible at the fibre surface. At the same time, some $Al_2MgC_2$ crystals have nucleated on impurity seeds located at the metal/fibre interface or close to it and begun to grow in the liquid. After 20 hours heating at 930 K (Fig. 11b), almost all the surface of the carbon fibres is wetted by the liquid alloy and the attack is much more severe than after 10 hours. Deep dissolution craters have formed at the fibre surface and new $Al_2MgC_2$ crystals have appeared. At this stage, it can be remarked that most of these $Al_2MgC_2$ crystals have developed in the vicinity of the fibre surface but not directly onto it. This indicates that the carbon surface is not a favourable site for the nucleation of $Al_2MgC_2$. After 75 hours heating at 930 K (Fig. 11c and d), more than one half of the initial carbon fibre has been dissolved and converted into $Al_2MgC_2$ crystals. As concerns these crystals, it is their size rather than their number that has increased between 20 and 75 hours heating, which account for the fairly different interface morphologies observed. When the nucleation sites initially present around the fibre were in sufficient number, the $Al_2MgC_2$ crystals have joined together and come in contact with the central part of the fibre not already attacked, forming the protective shell visible in Fig. 11c. When only few nucleation sites were initially present, some places of the carbon fibre still remain in direct contact with the liquid alloy and degradation by dissolution-precipitation can continue at a constant rate up to the complete consumption of the fibre, as shown in Fig. 11d.

The same experiments reproduced at 930 K with Mg-Al alloys containing 6 and 9 wt.% of aluminium led to nearly the same observations. The only differences that appeared when the aluminium content of the alloy increased were that the liquid alloy wetted the fibre surface at a slightly faster rate and that the $Al_2MgC_2$ crystals tended to develop closer to this surface. Comparison of Figs 11b, 12 and 13 illustrates these little differences at a reaction time of 20 hours. An EPMA concentration profile typical for these samples is shown in Fig. 14.

The effect of the fibre nature on the mechanism and kinetics of growth of $Al_2MgC_2$ can be seen on the SEM photographs taken after 20 hours heating at 930 K in a Mg-Al 6 alloy and presented in Figs 15 and 16. PAN-based M40 fibres (purity better than 99 wt.%C, 6.5 $\mu$m in diameter, Toray) were observed to react with Mg-rich Mg-Al alloys (Fig. 15) at the same rate and via the same dissolution-precipitation mechanism as pitch-based P55 fibres. This result can be understood by considering that in the two types of fibres, carbon is in about the same graphitization state with a crystallite size in the $c$ axis direction, $L_c$, in the order of 70–100 Å [10].

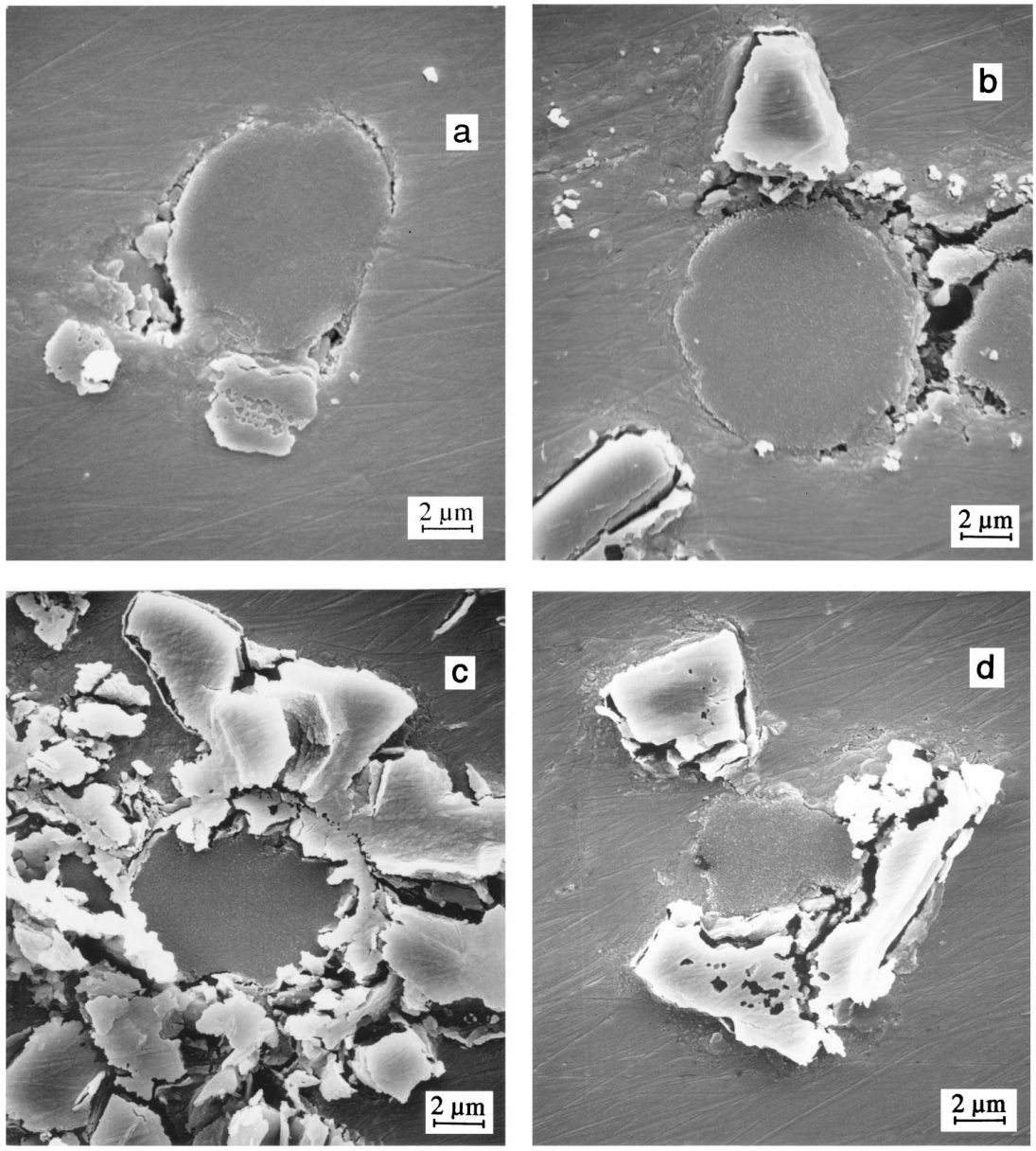


*Figure 11* Development of the interface reaction in Mg-Al 2.5/P55 samples heat-treated at 930 K. (a): for 10 hours; (b) for 20 hours; (c) and (d): for 75 hours.

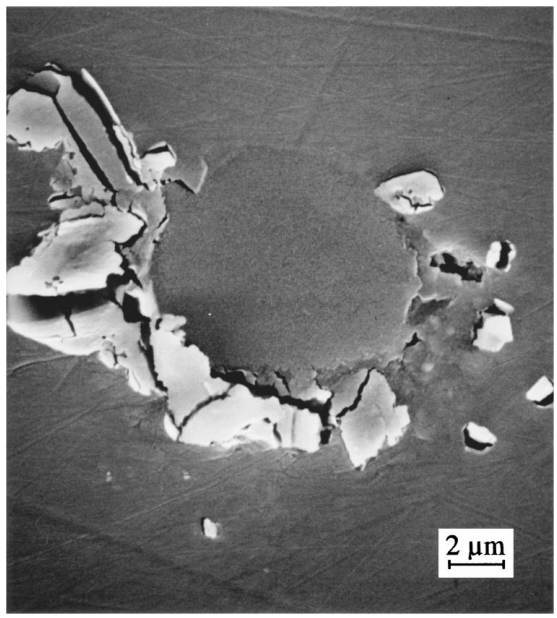


*Figure 12* Interface in a Mg-Al 6/P55 sample heat-treated at 930 K for 20 hours.

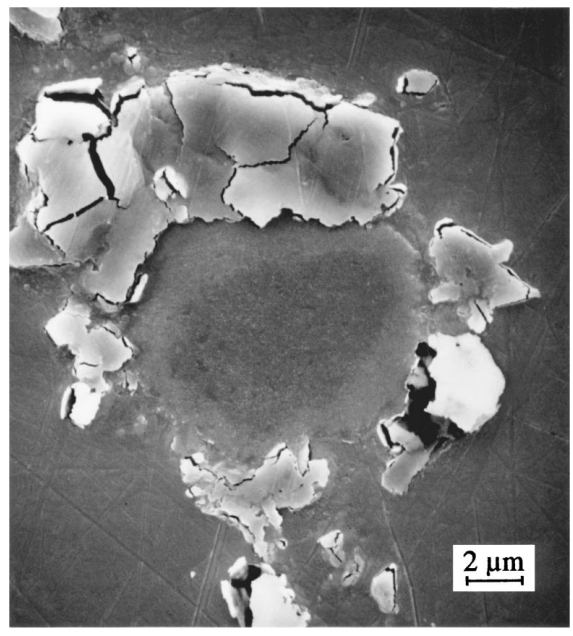


*Figure 13* Mg-Al 9/P55 sample heat-treated at 930 K for 20 hours.

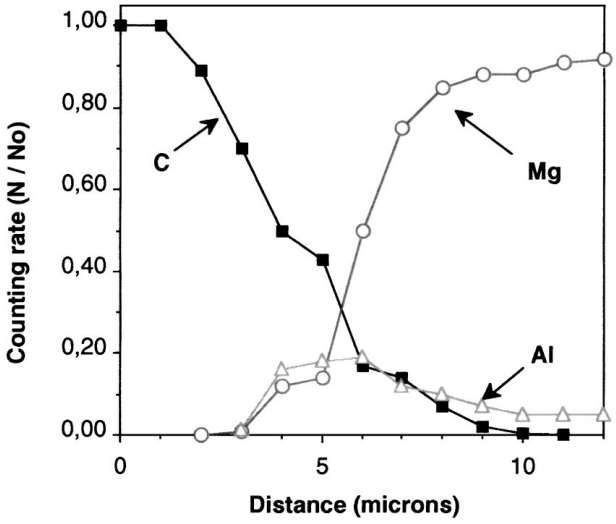


*Figure 14* EPMA concentration profiles recorded at the crossing of the interface in a Mg-Al 6/P55 sample heated for 20 hours at 930 K.

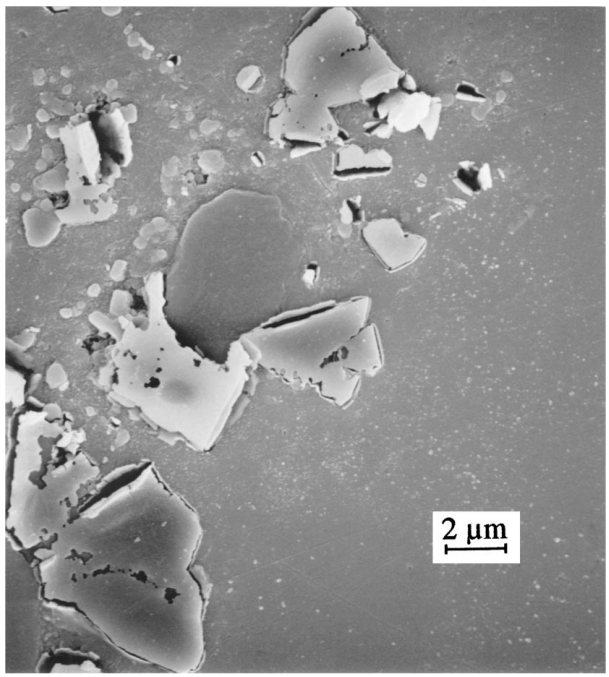


*Figure 15* Mg-Al 6/M40 interface after 20 hours heating at 930 K.

Consistently, highly graphitized pitch-based P100 fibres (purity better than 99 wt.%C, 10 $\mu$m in diameter, Amoco) with a $L_c$ value in the range 130–150 Å [10] appeared far less reactive than P55 or M40 fibres: no reaction could in effect be detected at the Mg-Al6/P100 interface after 20 hours heating at 930 K. As for the PAN-based T300 fibres (purity about 92 wt.%C, 7 $\mu$m in diameter, Toray), they exhibited a singular behaviour: they were the first of the four types to be wetted by the liquid Mg-Al alloy and to react with it, which was in agreement with their low degree of graphitization (Lc $\approx$ 10–20 Å) [10], but they were also the first to be passivated by a thin and continuous $Al_2MgC_2$ layer, as shown in Fig. 16. This rapid passivation might be related with the presence in the T300 fibres of 6–8 wt.% of nitrogen, which could give rise to the formation of $Mg_3N_2$ nucleation sites for $Al_2MgC_2$ at the metal/fibre interface.

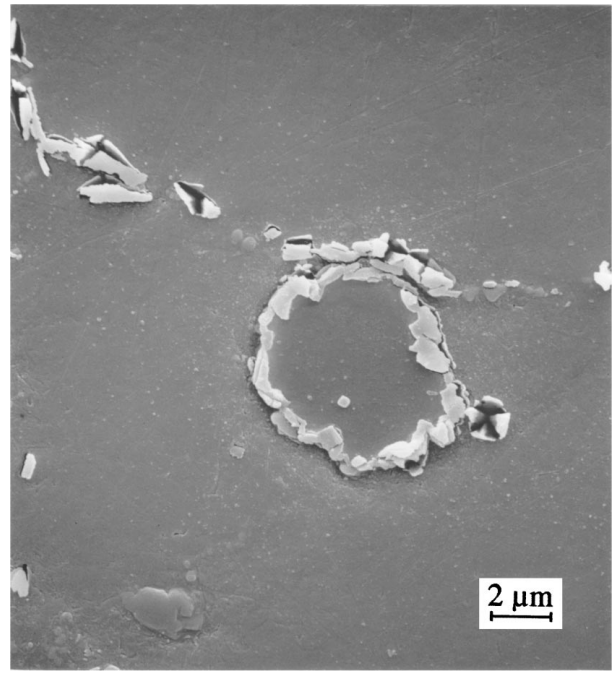


*Figure 16* Mg-Al 6/T300 interface after 20 hours heating at 930 K.

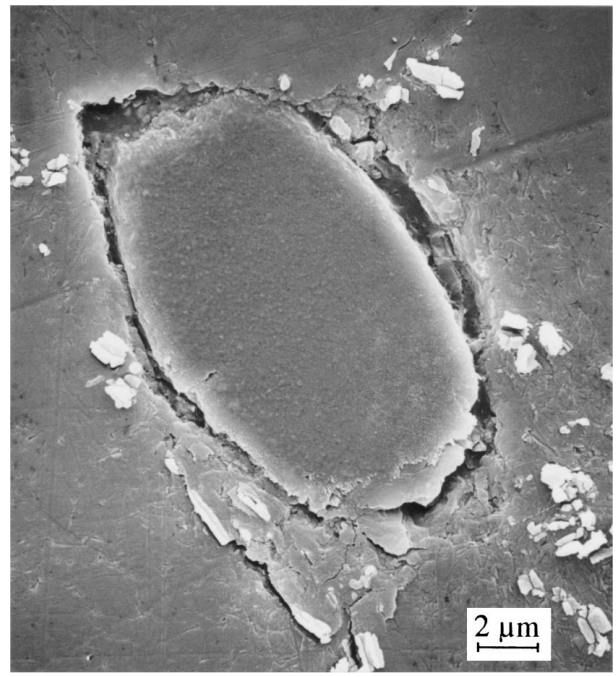


*Figure 17* Interaction between a P55 fibre and a Mg-Al 6 alloy in the semi-liquid state (860 K, 75 hours).

All the morphological features described above were not noticeably modified when the temperature was changed. In fact, what was strikingly modified was the rate at which the interaction process developed. As an example, complete dissolution of some P55 fibre pieces in a Mg-Al 2.5 alloy took less than 10 hours at 1000 K while at 930 K, more than 75 hours were necessary. At temperatures lower than 930 K, the reaction rate still decreased. As shown in Fig. 17, interaction between P55 fibres and a Mg-Al 6 alloy in the semi-liquid state had just begun after 75 hours heating at 860 K. $Al_2MgC_2$ crystals were also observed to form by dissolution-precipitation at the interface between P55 fibres and a

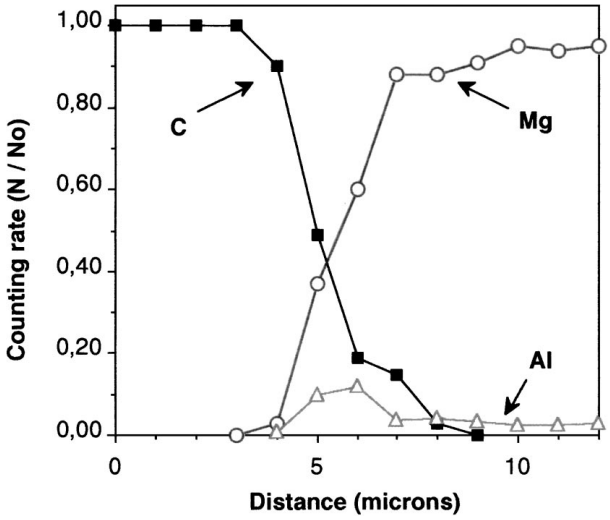


*Figure 18* EPMA concentration profile showing the presence of $Al_2MgC_2$ at the fibre/matrix interface in a Mg-Al 3/P55 sample heated for 1200 hours at 853 K.

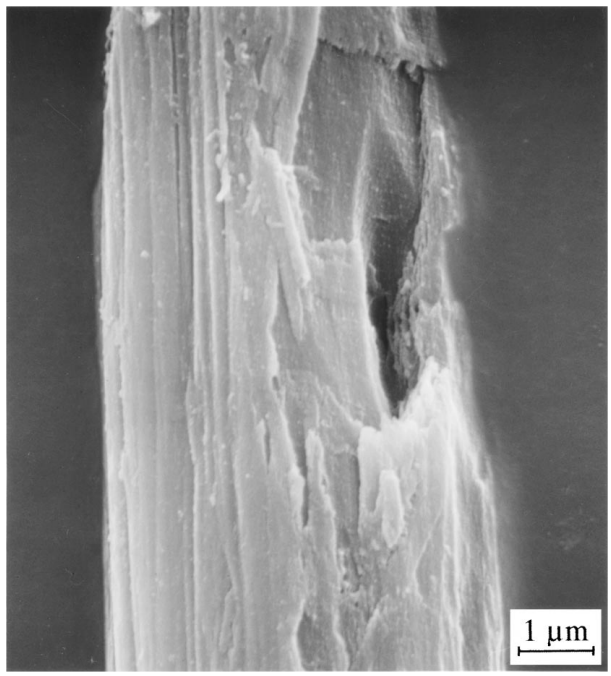


*Figure 19* Dissolution crater formed at the surface of a M40 fibre after 20 hours heating at 930 K in the presence of a Mg-Al 6 alloy (the metal matrix and $Al_2MgC_2$ were removed by acidic attack).

Mg-Al 3 alloy in the solid state at 853 K but in that case, the reaction progressed at a very slow rate, 1200 hours heating being necessary to characterize the ternary carbide $Al_2MgC_2$ by SEM (same interface morphology as that presented in Fig. 17) and by EPMA (Fig. 18).

Some experiments were finally carried out using the very common magnesium alloy AZ61 (6 wt.%Al, 1 wt.%Zn) instead of synthetic Mg-Al alloys. Neither zinc nor the other impurity elements present in the commercial alloy were observed to play a role in the reaction mechanism and kinetics. More especially, EPMA did not revealed any abnormal concentration of zinc or of the other impurity elements when approaching the alloy/fibre interface.

## 6. Conclusion

The aim of this study was to examine how the excellent chemical inertness of carbon fibres towards magnesium was affected when this metal was alloyed with aluminium. From the results obtained, it is clear that a chemical reaction can develop at the interface between carbon fibres and a Mg-Al alloy as soon as little amounts of aluminium are present in the alloy. At a temperature of 1000 K where all the Mg-Al alloys are in the liquid state, the aluminium content beyond which carbon can be attacked has been found to be of $0.6 \pm 0.2$ wt.%. This threshold value tends to increase with the temperature to attain at least 2.6 wt.% at 1273 K whereas for Mg-Al alloys in the solid state below 923 K, an interface reaction would still be possible for aluminium contents as low as 0.1 wt.%.

The products of the chemical interaction between carbon fibres and Mg-Al alloys are either the ternary carbide $Al_2MgC_2$ or the binary aluminium carbide $Al_4C_3$, depending on the composition of the alloy and on the temperature. At a temperature of 1000 K, $Al_2MgC_2$ is formed in Mg-Al alloys with an aluminium content ranging from 0.6 to $19 \pm 2$ wt.%Al and $Al_4C_3$ (with up to 6 wt.%Mg in solid solution) is produced in Mg-Al alloys with an aluminium content higher than $19 \pm 2$ wt.%Al.

Formation of $Al_2MgC_2$ by reaction between carbon fibres and Mg-rich Mg-Al alloys always proceeds via a dissolution-precipitation mechanism whatever the state of the alloy: liquid, semi-liquid or solid. This mechanism involves the migration of carbon atoms by diffusion in the alloy from the fibre surface where dissolution craters appear to the faces of $Al_2MgC_2$ crystals growing in the metal matrix. The rate at which interaction progresses mainly depends on the microstructure of the fibres (the most graphitized being the least reactive) and on the reaction temperature (thermally activated process). The alloy composition also influences the reaction kinetics but to a lesser extent.

From the practical point of view of processing magnesium base matrix composites reinforced with carbon fibres, the use of Mg-Al alloys instead of pure magnesium may be advantageous in several regards. It can for instance facilitate a better control of the infiltration and of the solidification of the metal matrix in composites produced by liquid phase processing [13]. It can also allow pre-coated fibre tapes to be consolidated by hot pressing in the semi-liquid state [22]. It is thought that these benefits will be kept as long as a chemical reaction at the metal/fibre interface will be avoided, which seems possible under certain processing conditions [12–14, 22], specially if highly graphitized fibres are used (observation made with P100 fibres in Section 5). On the other hand, it is considered that development of an interfacial reaction would rapidly be detrimental to the material properties. In effect, no improvement of interfacial wetting or bonding is to be expected from a reaction that proceeds via the dissolution-precipitation mechanism characterized while formation of dissolution craters at the fibre surface, as shown in Fig. 19, will rapidly constitute a grave source of damage.

## Acknowledgements

The authors gratefully acknowledge the CMEABG, Université Lyon 1, where characterizations by SEM and EPMA could be performed.

## References

1. A. P. LEVITT, E. DI CESARE and S. M. WOLF, *Metall. Trans.* **3** (1972) 2455.
2. P. ROY and A. MAMODE, in Proceedings of the 3rd Europ. Symp. on Spacecraft Materials in Space Environment, Noordwijk, The Netherlands, 1-4 Oct. 1985 (ESA SP-232, Nov. 1985), p. 185.
3. O. REMONDIERE, R. PAILLER, A. MAMODE and P. ROY, in Proceedings of the 1st Europ. Conf. on Composite Materials, edited by A. R. Bunsell, P. Lamicq and A. Massiah (AMAC, Bordeaux, 1989) p. 583.
4. D. B. EVANS and R. C. CLARIDGE, US Patent no. 5 353 981, 11 Oct. 1994.
5. L. CORNEC, Fr. Demande 2 698 582, 3 June 1994.
6. R. OAKLEY, R. F. COCHRANE and R. STEVENS, *Key Eng. Mater*., **104-107** (1995) 387.
7. E. G. WOLFF, B. K. MIN and M. H. KURAL, *J. Mater. Sci.* **20** (1985) 1141.
8. S. P. RAWAL, J. H. ARMSTRONG and M. S. MISRA, *Ceram. Eng. Sci. Proc.* **9** (1988) 1001.
9. J. C. VIALA, P. FORTIER, G. CLAVEYROLAS, H. VINCENT and J. BOUIX, in Proceedings of the 7th Europ. Conf. on Composite Materials, edited by A. R. Bunsell, P. Lamicq and A. Massiah (Elsevier, London, 1989) p. 583.
10. J. C. VIALA, P. FORTIER, G. CLAVEYROLAS, H. VINCENT and J. BOUIX, *J. Mater. Sci.* **26** (1991) 4977.
11. G. CLAVEYROLAS, Doctoral thesis no 156-91, University of Lyon, France, 1991.
12. S. P. RAWAL, L. F. ALLARD and M. S. MISRA in "Interfaces in Metal Matrix Composites," edited by A. K. Dhingra and S. G. Fishman (The Metallurgical Society of A.I.M.E., PA, 1986) p. 211.
13. M. RABINOVITCH, J. C. DAUX, J. L. RAVIART and R. MEVREL, in Proceedings of the 4th Europ. Conf. on Composite Materials, edited by J. Fueller (Elsevier, London, 1990) p. 405.
14. A. KLEINE, H. J. DUDEK and G. ZIEGLER, *ibid*. p. 267.
15. I. W. HALL, *Scr. Metall.* **21** (1987) 1717.
16. A. P. DIWANJI and I. W. HALL, in Proceedings of the 6th Int. Conf. on Composite Materials, edited by F. L. Matthews, N. C. R. Buskell, J. M. Hodgkinson and J. Morton (Elsevier, London, 1987) p. 2265.
17. S. J. SWINDLEHURST and I. W. HALL, in Proceedings of the Int. Symp. on Advances in Cast Reinforced Metal Composites, edited by S. G. Fishman and A. K. Dhingra (ASM International, Metals Park, OH, 1988) p. 281.
18. I. W. HALL, *J. Mater. Sci*. **26** (1991) 776.
19. C. BADINI, M. FERRARIS and F. MARCHETTI, Mater. Lett. **21** (1994) 55.
20. J. C. VIALA, F. BOSSELET, G. CLAVEYROLAS, B. F. MENTZEN and J. BOUIX, *Eur. J. Solid State Inorg. Chem*. **28** (1991) 1063.
21. T. B. MASSALSKI, "Binary Alloy Phase Diagrams, Vol. 1" (American Society for Metals, Metals Park, OH, 1986) p. 129.
22. L. SCHEED, Doctorat thesis no 2221, Paris-Orsay, France, 1992.

*Received 12 February 1997*
*and accepted 25 August 1999*